ChemistrySelect

Research Article
doi.org/10.1002/slct.202203140

Chemistry Europe
European Chemical Societies Publishing

www.chemistryselect.org

Trinitro-orcinolate and Trinitro-resorcinate – Sensitivity Trends in Nitroaromatic Energetic Materials**

Simon M. J. Endraß, Andreas Neuer, Thomas M. Klapötke, and Jörg Stierstorfer*[a]

5-Methyl-2,4,6-trinitrobenzene-1,3-diol (trinitro-orcinol, H_2TNO) as a close structural relative to the well-known energetic materials trinitroresorcinol (styphnic acid) and trinitrotoluene (TNT) is prepared in high purity and analyzed concerning its vapor pressure using the transpiration method. Several energetic coordination compounds (ECCs) of its respective anion were produced and compared with structurally close styphnate complexes to give an insight into physiochemical trends of the ECC. The synthesized compounds were further analyzed by elemental analysis, IR spectroscopy, differential thermal analysis and low temperature X-ray diffraction analysis. To classify the reported compounds among the energetic materials, they were tested for their sensitivities towards mechanical stimuli such as impact, friction and electrostatic discharge as well as their behavior towards flame.

Introduction

Nitroaromatic compounds can be found in multiple industries and applications for example as drugs, dyes, pesticides and energetic materials.[1,2] Therefore, these compounds are distributed throughout the whole ecosystem and by various sources despite their well-known structure-toxicity relationship.[3–5] This is problematic as many compounds of this kind have been proven to be persistent in soil and are degraded within long time spans by different species.[6–8] Within the field of energetic materials, various nitroaromatic compounds have been studied and commonly found application as the oxidation of the carbon backbone can create interesting physiochemical properties.[9–11] By variation of the structural motifs and formation of salts and coordination compounds (Figure 1), different fields of application of the energetic materials have been achieved depending on the performance and sensitivities of the compounds.[12–14] However, this structural variety also leads to the necessity of methods for detection in order to provide safety precautions to civilians and military.[15,16]

Often, the detection and possibilities for sample processing are limited by the type of design and exact way of application of the ordnance which might only allow measurement of the vapor pressure.[19,20] Trinitro-orcinol (H_2TNO) has been known since the 1870s but despite its structural similarities with styphnic acid (H_2TNR) and trinitro-toluene (TNT) it was not considered a potential energetic material.[21,22] This changed when in 2016 this group published first results of H_2TNO and the formation of its energetic salt Cs_2TNO.[23,24] Preliminary flame tests and the information that H_2TNO could serve as a potential starting material for primary explosives was described. However, no information on the initiation performance and potential application were given. In order to provide possible trends of energetic salts and coordination compounds the goal of this work was to synthesize and characterize several compounds and compare them with literature known styphnate compounds. Furthermore, neat trinitro-orcinol was evaluated concerning its vapor pressure to deliver an additional safety aspect of detection.

Results and Discussion

Synthesis

Trinitro-orcinol (**1**) was prepared by nitration of commercially available orcinol (5-methylbenzene-1,3-diol) as described in the literature (Scheme 1).[25] The nitration can be performed under relatively mild conditions leading to high yields due to the activating effect of the hydroxy groups.[26]

The obtained H_2TNO was further reacted in acid-base reactions (Scheme 2) which led to aqueous solutions of the respective salts (basic copper carbonate, zinc carbonate, cesium

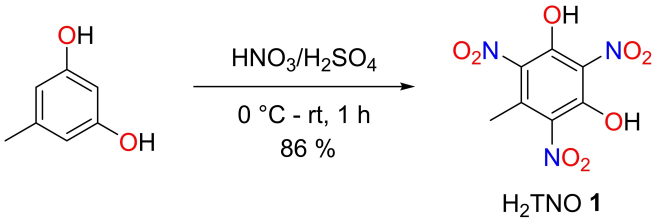

H_2TNO **1**

Scheme 1. Preparation of trinitro-orcinol (H_2TNO).

[a] *S. M. J. Endraß, A. Neuer, Prof. Dr. T. M. Klapötke, Dr. J. Stierstorfer*
Energetic Materials Research, Department of Chemistry
Ludwig Maximilian University Munich
Butenandtstr. 5–13, 81377
Munich, Germany
E-mail: jstch@cup.uni-muenchen.de
Homepage: www.hedm.cup.uni-muenchen.de/index.html

[**] *Parts of this work were published on the NTREM 2022 conference.*[44,45]

Supporting information for this article is available on the WWW under https://doi.org/10.1002/slct.202203140

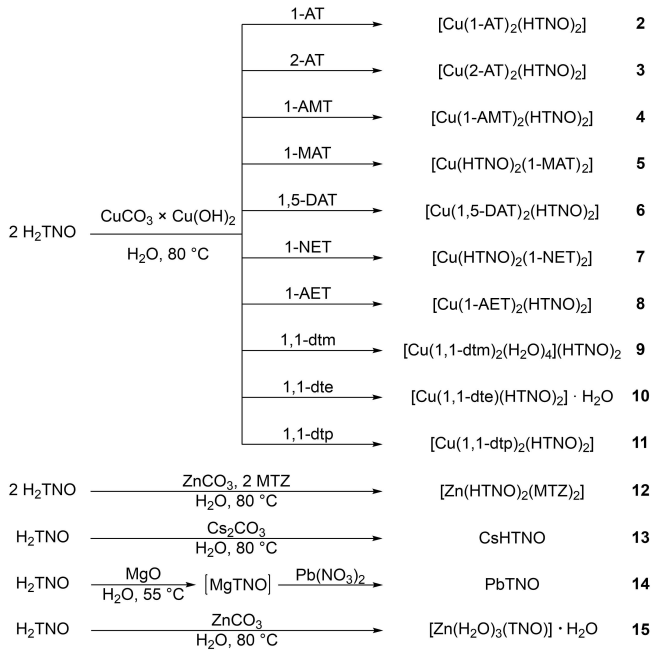

Scheme 2. Complexation and formation of salts of H_2TNO.

carbonate or magnesium oxide). These solutions were left to crystallize at room temperature to obtain the salts or used for complexation. Apart from compounds **4**, **9**, **10**, **12** and **14** single crystals suitable for X-ray diffraction analysis were obtained from the mother liquor. Compounds **9** and **12** were recrystallized from EtOH at room temperature to isolate single crystals of the compounds.

In the case of PbTNO, the synthetic approach of the commonly used β-lead styphnate was applied.[27] For this matter, MgO was added to a suspension of H_2TNO in water at 55 °C. The resulting solution was filtered off and lead(II) nitrate was added, which led to precipitation of the product.

In addition, three previously unknown styphnate complexes were prepared to compare them with trinitro-orcinolate complexes that carry the same ligand. In the case of the 1,5-diaminotetrazole (1,5-DAT) ligand, a styphnate complex was described in the literature, however the sensitivity determination was carried out according to a different standard which is not comparable.[28] Instead of the literature-known $[Cu(1,5\text{-}DAT)_2(HTNR)_2]$, the double deprotonated styphnate species $[Cu(1,5\text{-}DAT)_2(TNR)]$ was obtained in all attempts of preparation. An overview over the prepared styphnate complexes is given in Scheme 3.

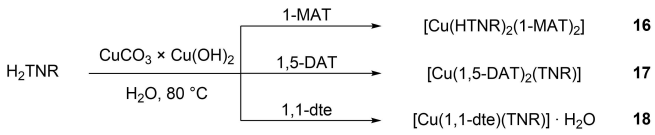

Scheme 3. Preparation of styphnate complexes **16**–**18**.

Vapor pressure

The experimental vapor pressures p_{sat} as well as the thermochemical properties such as molar enthalpies of sublimation $\Delta_{cr}^{g}H_{m}^{\circ}(T)$ and molar entropies of sublimation $\Delta_{cr}^{g}S_{m}^{\circ}(T)$ of H_2TNO was determined using the transpiration method with coupled quantification via high pressure liquid chromatography assisted by an UV-diode array detector (HPLC-DAD) and was categorized in the existing literature of related nitroaromatics (H_2TNR, TNT).[29,30] Here, the data acquisition was obtained from a complete *p-T* dataset with an elaborate calculation based on the *Clausius-Clapeyron* equation.[31] The extrapolation to the standard temperature T_{ref} was carried out by the application of the modified *Clarke-Glew* fit function (see Supporting Information).

This technique allowed the determination of the sublimation behavior of H_2TNO in the temperature range of 332.4–380.7 K (for further information see Supporting Information). The absolute vapor pressures p_{sat} and thermodynamic properties of sublimation including the *Clark-Glew* fit function were presented in Table S8 of the ESI. From these results, the molar enthalpy of sublimation was found to be $122.7 \pm 1.7\ kJ\,mol^{-1}$ and the extrapolated vapor pressure at reference temperature of 298.15 K was derived to be 7.27 μPa.

Since this work determined the appointed thermochemical properties for the first time, the substance H_2TNO was contextualized to the related compounds H_2TNR and TNT. To enable a suitable comparison, the existing literature data were processed in the same manner as described in this paper. For this purpose, the revised properties were presented in Table 1 and Figure 2.

The vaporization behavior of H_2TNR was measured by *Cundall* in the temperature range of 330.2–440.9 K.[30] The molar enthalpy of sublimation was found to be $124.5\ kJ\,mol^{-1}$ and from these findings the vapor pressure at reference temperature of 298.15 K (6.66×10^{-4} μPa) was extrapolated based on a calculated *p-T* data set via the published *Clausius-Clapeyron* equation and the application of the *Clark-Glew* fit function together with the calculated molar heat capacity (see Table S7).

In addition, the vaporization behavior of TNT was measured by *Cundall* and revised by *Östmark*.[29,30] The reported *Antoine* equation was determined in the temperature range of 285.1–353.4 K and converted into the *Clarke-Glew* fit function considering the molar heat capacity (see Table S7). The molar enthalpy of sublimation was found to be $114.1\ kJ\,mol^{-1}$ and from these findings the vapor pressure at reference temperature of 298.15 K (714 μPa) were extrapolated.

By contrasting H_2TNO, the volatility was found to settle in between the two comparative substances H_2TNR and TNT. Thus, H_2TNO has a volatility four orders of magnitude higher than H_2TNR and a volatility two orders of magnitude lower than TNT. In addition, the sublimation enthalpy changes marginally compared to H_2TNR and by around $10\ kJ\,mol^{-1}$ compared to TNT. Also, the illustrated fit function (see Figure 2) indicates that the slope of the fit functions approximates and the offset decreases from TNT over H_2TNO to H_2TNR. This classification corroborates our research results, since in an

Table 1. Comparison of thermodynamic properties of the compounds H_2TNR, H_2TNO and TNT: Vapor pressure p_{sat} and molar enthalpies of sublimation $\Delta_{cr}^{g}H_{m}^{\circ}$ at 298.15 K.

Experiment	*T*-Range K	$\Delta_{cr}^{g}H_{m}^{\circ}$(298.15 K)[a] kJ mol^{-1}	p_{sat}[b] µPa
H_2TNO	332.4–380.7	122.7 ± 1.7 [c]	7.27
H_2TNR[30]	330.2–440.9	124.5	6.66 ×10^{-4}
TNT [29]	285.1–353.4	114.1	714

[a] Molar enthalpies of sublimation were adjusted according to *Chickos et al.* [32] with values of $\Delta_{cr}^{g}C_{p,m}^{\circ}$, $C_{p,m}^{\circ}$(cr) stated in Table S7. [b] Vapor pressure at 298.15 K extrapolated from the *p*-*T*-data. [c] Uncertainties for molar enthalpies of sublimation at reference temperatures are expressed as expanded uncertainties with confidence level of 0.95 (k = 2).

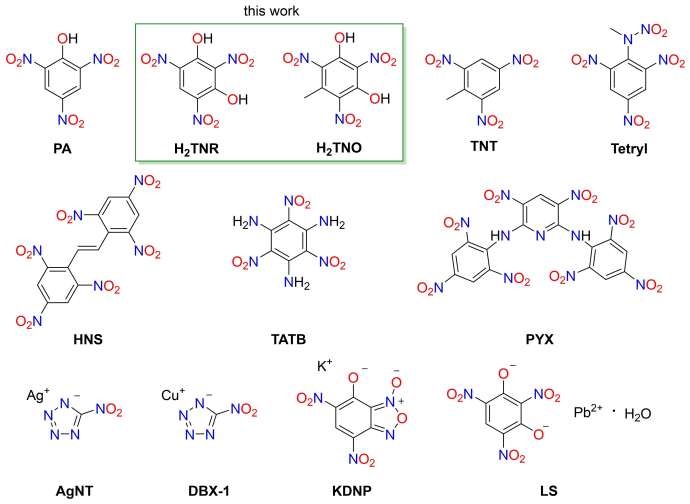

Figure 1. Overview of few examples of nitroaromatic energetic materials for different fields of application:[17,18] PA: picric acid, H_2TNR: styphnic acid, TNT: trinitrotoluene, HNS: hexanitrostilbene, TATB: 1,3,5-triamino-2,4,6-trinitrobenzene, PYX: 2,6-Bis(picrylamino)-3,5-dinitropyridine, AgNT: silver(I) 5-nitrotetrazolate, DBX-1: copper(I) 5-nitrotetrazolate, KDNP: potassium 5,7-dinitro-[2,1,3]-benzoxadiazol-4-olate 3-oxide, LS: lead styphnate.

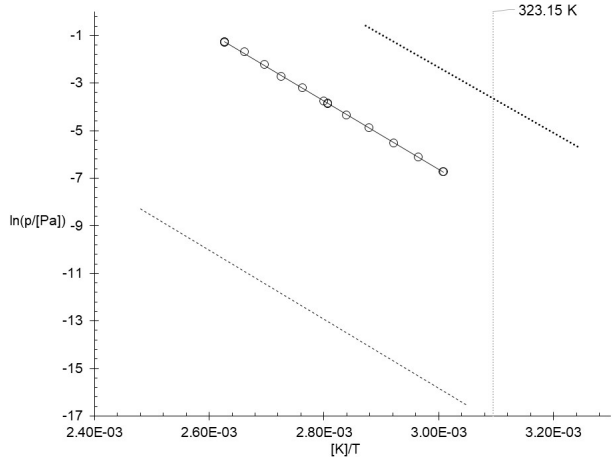

Figure 2. Comparison of the experimental vapor pressure values with the *Clausius-Clapeyron* fit function of the investigated H_2TNO with the corresponding published fit function of H_2TNR and TNT. Here ○ and solid line is H_2TNO; dashed line is H_2TNR; dotted line is TNT. The vertical dotted line serves merely as a guide.

analogous way as the volatility, polarity can also be lined up: H_2TNR has the highest polarity in comparison and TNT the lowest. Since a higher polarity has a direct demeaning effect on the volatility, it can be argued that the particular volatility of H_2TNO is plausible. Moreover, it can be observed that a similar fit function slope can be expected for related substances. Based on these considerations and the assured reproducibility of the measured values (procedure described in previous publications), we have a high degree of confidence in the determined values and have gained access to the thermochemical properties for the first time.

Detonation properties

The energetic properties of compound **1** are calculated with EXPLO5 program code and are displayed in Table 2.[33] Therefore, the enthalpy of formation was determined by applying the atomization method using room temperature CBS-4 M enthalpy and the experimentally determined molar enthalpy of sublimation. For better comparability, the properties of styphnic acid and TNT were recalculated using the same version of EXPLO5. Additionally, CBS-4 M results of all three substances are given in the Supplementary Information. Especially the detonation pressure at the *Chapman-Jouguet* point and the

Table 2. Energetic properties of H_2TNO compared to H_2TNR and TNT.

	H_2TNO (1)	H_2TNR [34]	TNT [34]
Formula	$C_7H_5N_3O_8$	$C_6H_3N_3O_8$	$C_7H_5N_3O_6$
M [g mol^{-1}]	259.13	245.10	227.13
ρ [g cm^{-3}]	1.71[a]	1.83	1.65
N [%][b]	16.22	17.14	18.50
Ω_{CO} [%][c]	−9.3	3.3	−24.7
$\Delta_f H°$ [kJ mol^{-1}][d]	−436.7[i,k]	−374.3[i]	−59.3
Explo5 V6.05.04			
$-\Delta_{Ex}U$ [kJ kg^{-1}][e]	4024	4509	4406
$T_{det.}$ [K][f]	3026	3391	3177
V_0 [L kg^{-1}][g]	637	626	640
P_{CJ} [kbar][h]	198	252	183
$V_{det.}$ [m s^{-1}][i]	6987	7668	6798

[a] From X-Ray diffraction analysis recalculated to 298 K. [b] Nitrogen content. [c] Oxygen balance with respect to CO. [d] Enthalpy of formation. [e] Energy of explosion. [f] Detonation temperature. [g] Volume of detonation products (assuming only gaseous products). [h] Detonation pressure at the *Chapman-Jouguet* point. [i] Detonation velocity. [j] calculated by CBS-4M and atomization method; [k] corrected by gas-phase measurement.

detonation velocity correspond very well to the structural similarities of the compounds.

Crystal Structures

Compounds **2**, **3**, **5**–**9**, **11**–**13** and **15** were further examined by low-temperature X-ray diffraction analysis. The data and parameters of the measurements as well as the refinements are given in the supporting information Tables S1–4. [Cu(1-AT)$_2$(HTNO)$_2$] crystallizes in the monoclinic space group $P2_1/c$ with a calculated density of 1.90 g cm^{-3} at 101 K and two formula units per unit cell. The compound shows the typical *Jahn-Teller*-like distortion (Figure 3) of a d^9-metal center in octahedral coordination as expected for Cu^{2+}. The distorted axis is formed by the coordinating nitro groups of the trinitro-orcinolate anions, while the coordination bonds, that are formed by the deprotonated hydroxy group and the 1-amino-5*H*-tetrazole ligand are significantly shorter.

The comparison of this coordination pattern, however, reveals a significant difference compared to the styphnate anions that is displayed in Figure 4. While the styphnate anions are known to coordinate via the nitro groups in *ortho*-position to the remaining proton of the carbon backbone, nitro group that is involved in the coordination of trinitro-orcinolate, is in *para*-position to the methyl group. This coordination pattern is also observed for the ECCs **3**, **5**, **6**, **7**, **8** and **12**. The crystal structures of compounds **3** and **5**–**8** can be found in the Supplementary Information.

[Cu(1,1-dtm)$_2$(H$_2$O)$_4$](HTNO)$_2$ crystallizes in the triclinic space group $P-1$ with a density of 1.78 g cm^{-3} at 173 K. Unlike in the literature known styphnate complex [Cu(1,1-dtm)(TNR)]·H$_2$O neither the anion nor the 1,1-dtm ligand showed bridging behavior in the case of compound **9**.[36] Instead, a composition close to the respective picrate complex was observed as displayed in Figure 5. The $HTNO^-$ anion is pushed out of the

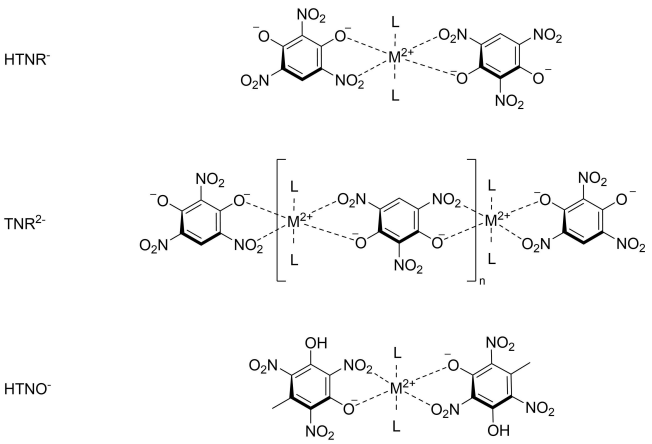

Figure 4. Typical coordination pattern of the styphnate anions $HTNR^-$ and TNR^{2-} in ECCs compared to $HTNO^-$.[35]

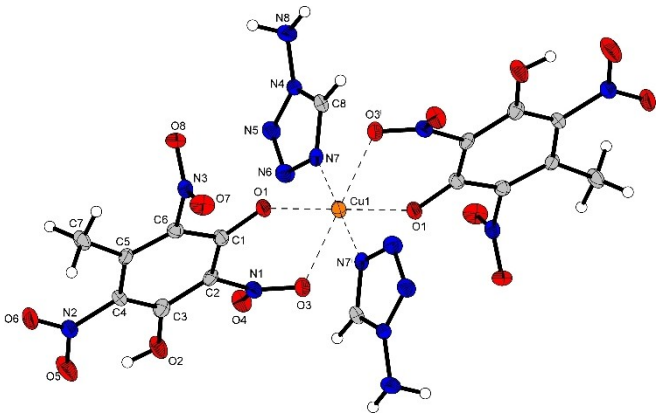

Figure 3. Crystal Structure of [Cu(1-AT)$_2$(HTNO)$_2$] with typical structural motif. Selected bond lengths (Å): Cu1–O1 1.959(3), Cu1–O3 2.355(3), Cu1–N7 2.002(4); selected bond angles (°): O1–Cu1–O3 79.61(12), O1–Cu1–N7 88.98(15), O3–Cu1–N7 94.64(14); symmetry codes: (i) 1 − x, 1 − y, 1 − z.

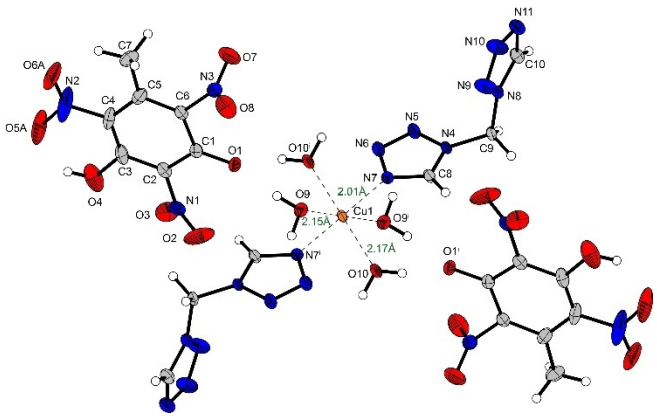

Figure 5. Crystal Structure of [Cu(1,1-dtm)$_2$(H$_2$O)$_4$](HTNO)$_2$. Selected bond lengths (Å): Cu1–O9 2.153(3), Cu1–O10 2.177(3), Cu1–N7 2.007(3); selected bond angles (°): O9–Cu1–O10 90.60(11), O9–Cu1–N7 91.08(13), O10–Cu1–N7 86.76(13); symmetry codes: (i) 1 − x, 1 − y, 1 − z.

coordination sphere of the copper(II) center and replaced by four molecules of water. Therefore, the metal center is still coordinated octahedrally, but unlike expected without the more common *Jahn-Teller*-like elongation distortion of the coordination sphere. Instead, the four molecules of water are close to evenly distributed with coordination bond lengths of 2.15–2.17 Å and a compressed axis with a Cu^{2+}-ligand distance of 2.01 Å resulting in a *Jahn-Teller*-like compression distortion.

The X-ray diffraction analysis of compound **11** (Figure 6) reveals the distorted octahedral coordination of the copper(II) center by two molecules of ligand and anion each. The elongated axis is taken up by the deprotonated hydroxide of the trinitro-orcinolate, while the xy-level of the octahedra is occupied by the lateral nitrogen atoms of both tetrazole rings. Therefore, no coordination by the nitro group is possible. The compound crystallizes in the monoclinic space group $P2_1/c$ with a density of 1.77 g cm^{-3} at 173 K and two formula units per unit cell.

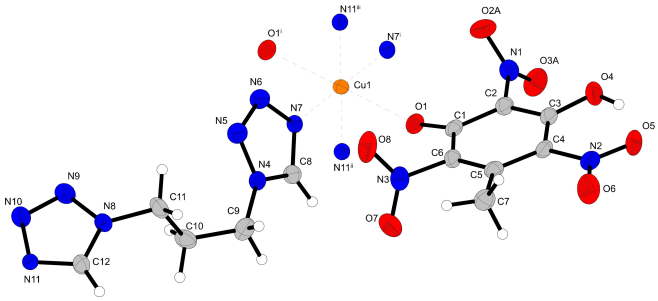

Figure 6. Asymmetric unit of $[Cu(1,1\text{-dtp})_2(HTNO)_2]$. Selected bond lengths (Å) O1–Cu1 2.3426(17), N7–Cu1 1.9956(15), N11–Cu1 2.0232(15); selected bond angles (°): N7–Cu1–N11^{ii} 90.54(6), N7–Cu1–O1 86.65(6), O1–Cu1–N11^{ii} 85.72(6); symmetry codes: (i) 2 − x, 1 − y, 1 − z; (ii) 1 + x, 1/2 − y, 1/2 + z; (iii) 1 − x, 1/2 + y, 1/2 − z.

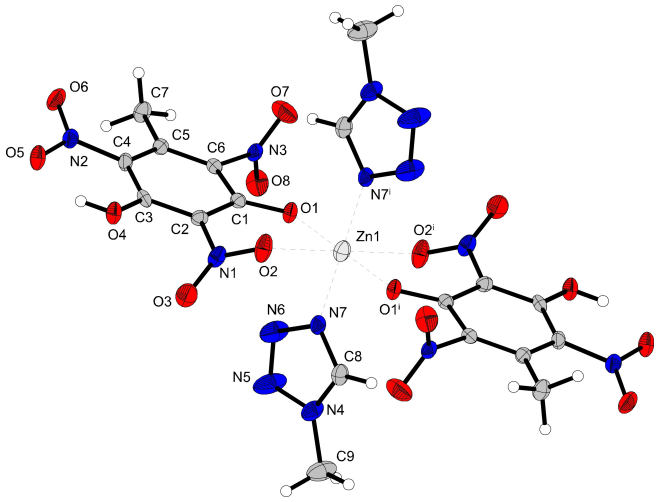

Figure 7. Crystal structure of $[Zn(HTNO)_2(MTZ)_2]$. Selected bond lengths (Å) Zn1–O1 1.940 (2), Zn1–O2 2.371(3), Zn1–N7 1.995(3); selected bond angles (°): O1–Zn1–O2 81.31(9), O1–Zn1–N7 89.32(11), O2–Zn1–N7 88.66(11); symmetry codes: (i) 1 − x, 1 − y, 2 − z.

As displayed in Figure 7, $[Zn(HTNO)_2(MTZ)_2]$ shows the typical coordination pattern of the trinitro-orcinolate anion that was shown earlier. The compound crystallizes in the triclinic space group *P*-1 with a density of 1.83 g cm^{-3} at 98 K.

Figure 8 shows a representative of the double deprotonated anion TNO^{2-} in form of the coordination compound $[Zn(H_2O)_3(TNO)]\cdot H_2O$. The crystal structure indicates, that unlike the styphnate anion TNR^{2-}, no 1D-polymeric chains are formed by TNO^{2-}. Instead of a symmetric coordination by both hydroxides, the torsion angles of the nitro groups lead to a low symmetry coordination pattern. While the coordinating nitro group in *ortho*-position to methyl group shows a torsion angle of −28.4(4)° (O5–N2–C4–C3), the noncoordinating nitro group in *ortho*-position is twisted further to an angle of 67.2(4)° (O8–N3–C6–C1).

Physiochemical properties

The thermal behavior of all compounds was investigated via differential thermal analysis (DTA) in a range of 25–400 °C with a heating rate of 5 °C min^{-1}. The observed events were given as onset temperatures. Endothermic events (e.g. melting point, loss of water or ligand, phase transition) were further investigated by thermogravimetric analysis (TGA) at a similar heating rate in the range 30–400 °C. Plots of every DTA measurement as well as TGA can be found in the supporting information. Detail on the cause of the endothermic events as well as the exothermic decomposition temperatures are briefly given in Table 3. The reported sensitivities classify all com-

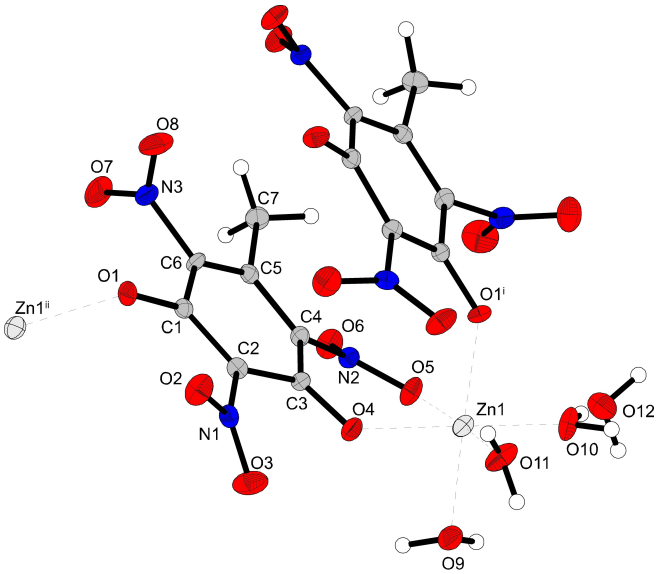

Figure 8. Crystal structure of compound **15**. Selected bond lengths (Å): Zn1–O1^{i} 2.073(2), Zn1–O4 2.028(2), Zn1–O5 2.123(3), Zn1–O9 2.123(2), Zn1–O10 2.039(3), Zn1–O11 2.062(3); selected bond angles (°): O1^{i}–Zn1–O9 175.07(12), O1^{i}–Zn1–O4 94.55(9), O1^{i}–Zn1–O5 92.13(11), O1^{i}–Zn1–O10 89.09(10), O1^{i}–Zn1–O11 86.57(11), O9–Zn1–O488.45(9), O9–Zn1–O5 84.50(11), O9–Zn1–O10 87.36(10), O9–Zn1–O11 97.19(12), O4–Zn1–O5 80.32(9), O4–Zn1–O11 93.09(10), O5–Zn1–O12 90.8(1), O11–Zn1–O12 95.89(11), O4–Zn1–O10 170.5(1), O5–Zn1–O11 173.17(10); symmetry codes: (i) 1/2 + x, 1/2 − y, z, (ii) − 1/2 + x, 1/2 − y, z.

Table 3. Thermal Stability[a] and sensitivities to mechanical and electrical stimuli of compounds **2**–**14**, compared to literature known styphnates.

Compound	T_{endo}[b] [°C]	T_{exo}[c] [°C]	*IS*[d] [J]	*FS*[e] [N]	*ESD*[f] [mJ]	*HP*[g]	*HN*[h]
$[Cu(1\text{-}AT)_2(HTNO)_2]$ **2**	–	185	< 1	96	50	def.	dec.
$[Cu(1\text{-}AT)_2(HTNR)_2]$[35]	–	186	1.5	48	16	def.	def.
$[Cu(2\text{-}AT)_2(HTNO)_2]$ **3**	–	182	< 1	80	50	def.	def.
$[Cu(2\text{-}AT)_2(HTNR)_2]$[35]	–	206	3	48	20	def.	def.
$[Cu(1\text{-}AMT)_2(HTNO)_2]$ **4**	–	192	< 1	60	250	def.	dec.
$[Cu\ (1\text{-}AMT)_2(TNR)]$[35]	–	212	2	16	6.3	def.	def.
$[Cu(HTNO)_2(1\text{-}MAT)_2]$ **5**	–	220	2	> 360	90	def.	dec.
$[Cu(HTNR)_2(1\text{-}MAT)_2]$ **16**	–	249	2	> 360		def.	dec.
$[Cu(1,5\text{-}DAT)_2(HTNO)_2]$ **6**	–	220	< 1	360	200	def.	dec.
$[Cu(1,5\text{-}DAT)_2(HTNR)_2]$[28]	–	242	1.5[i]	-[i]	n.d.	n.d.	n.d.
$[Cu(1,5\text{-}DAT)_2(TNR)]$ **17**	–	229	< 1	45	160	def.	dec.
$[Cu(HTNO)_2(1\text{-}NET)_2]$ **7**	–	159	< 1	192	90	def.	dec.
$[Cu(1\text{-}NET)_2(TNR)]$ [38]	–	195	2	96	480	def.	def.
$[Cu(1\text{-}AET)_2(HTNO)_2]$ **8**	–	191	< 1	> 360	90	def.	dec.
$[Cu(1\text{-}AET)_2(TNR)]$[39]	–	177	< 1	240	123	def.	def.
$[Cu(1,1\text{-}dtm)_2(H_2O)_4](HTNO)_2$ **9**	100[j]	197	< 1	360	160	dec.	dec.
$[Cu(TNR)(1,1\text{-}dtm)]\cdot H_2O$[36]	–	236	2	192	188	def.	dec.
$[Cu(1,1\text{-}dte)(HTNO)_2]\cdot H_2O$ **10**	–	252	> 40	192	200	def.	dec.
$[Cu(1,1\text{-}dte)(TNR)]\cdot H_2O$ **18**	–	264	20	360	200	def.	def.
$[Cu(1,1\text{-}dtp)_2(HTNO)_2]$ **11**	–	184	< 1	240	200	def.	dec.
$[Cu(1,1\text{-}dtp)(TNR)]\cdot H_2O$[40]	88 ($-H_2O$)	248	10	> 360	500	n.d.	n.d.
$[Zn(HTNO)_2(MTZ)_2]$ **12**	–	229	2	168	33	def.	dec.
$[Zn(HTNR)_2(MTZ)_2]$[41]	–	214	4	240	800	n.d.	n.d.
CsHTNO **13**	–	233	< 1	> 360	50	def.	det.
$[Cs_2(H_2O)(HTNR)(OH)]_n$[42]	74 ($-2\ H_2O$)	292	–	–	–	n.d.	n.d.
PbTNO **14**	–	240	< 1	< 0.1	0.54	det.	det.
LS [34,43]	–	282	8	0.45	0.9	det.	det.

[a] DTA onset temperatures at a heating rate of 5 °C min^{-1}. [b] Onset temperature of endothermic event in the DTA, indicating a melting point of the compound. [c] Onset of exothermic event in the DTA. [d] Impact sensitivity (BAM drophammer (1 of 6)). [e] Friction sensitivity (BAM friction tester (1 of 6)). [f] Electrostatic discharge devise (OZM XSpark10). [g] Hot plate test (det.: detonation, def.: deflagration, dec.: decomposition, n.d.: not determined). [h] Hot needle test (det.: detonation, def.: deflagration, dec.: decomposition, n.d.: not determined). [i] according to China National Military Standard.[28] [j] gradual loss of mass.

pounds except of **10** (insensitive) and **18** (sensitive) as very sensitive towards impact according to the "UN Recommendations on the Transport of Dangerous Goods".[37] Furthermore, compounds **5**, **8**, **13** are considered insensitive towards friction, while **6**, **9**, **18** are less sensitive. Compounds **2**, **7**, **10**, **11** and **12** have been tested to be sensitive, **3**, **4**, **17** are very sensitive and only compound **14** is characterized as extremely sensitive towards friction. The general trend seems to be an increased impact sensitivity as well as lowered friction sensitivity and thermal stability of the trinitro-orcinolate complexes compared to the respective styphnates.

Conclusion

This work has provided 17 new compounds, among which 11 were characterized by low-temperature X-ray diffraction analysis. This analysis gave an interesting insight in the coordination behavior of trinitro-orcinolate compared to the anions of styphnic acid. Surprisingly, the investigation of the physiochemical properties showed, that despite the lower enthalpy of formation, trends towards an increased impact sensitivity and lower thermal stability of the trinitro-orcinolates can be observed. The sensitivities towards friction, in contrast, seem followed to be lower compared to the respective styphnates. In addition, the experimental vapor pressure of H_2TNO was determined, using the transpiration method. This crucial parameter for explosives' detection was put in context by comparison with literature values of the close structural relatives trinitroresorcinol and trinitrotoluene. The observed similarities of the fit function slopes as well as the overall placement of the volatility in between the literature values plausibly represent the shared structural similarities. While the high sensitivities towards impact, that were observed for most trinitro-orcinolates, excludes them from application as a primary explosive, utilization as a replacement of lead styphnate or as a sensitizer in priming mixtures might be considered.

Supporting information

Supplementary data on synthesis, purity assessment of the compounds and details of the quantification methods are provided in the Supporting information.

Deposition Number(s) 2191773 (for **2**), 2191776 (for **3**), 2191775 (for **5**), 2191782 (for **6**), 2191777 (for **7**), 2191778 (for **8**), 2191779 (for **9**), 2191774 (for **11**), 2191783 (for **12**), 2191781 (for **13**) and 2191780 (for **15**) contain the supplementary crystallographic data for this paper. These data are provided

free of charge by the joint Cambridge Crystallographic Data Center and Fachinformationszentrum Karlsruhe Access Structures service.

Acknowledgements

For financial support of this work by Ludwig-Maximilian University (LMU), the Office of Naval Research (ONR) under grant no. ONR N00014-19-1-2078 and the Strategic Environmental Research and Development Program (SERDP) under contract no. W912HQ19C0033 and the DAAD (German Academic Exchange Service) [grant no. 57299294] are gratefully acknowledged. The authors would like to thank Dr. Burkhard Krumm for NMR measurements and Kay Chen for proofreading. Open Access funding enabled and organized by Projekt DEAL.

Conflict of Interest

The authors declare no conflict of interest.

Data Availability Statement

The data that support the findings of this study are available in the supplementary material of this article.

Keywords: Crystal Engineering · Energetic Coordination Compounds · Energetic Materials · Experimental Vapor Pressure · Structure Elucidation

[1] K.-S. Ju, E. Parales Rebecca, *Microbiol. Mol. Biol. Rev.* **2010**, *74*, 250–272.
[2] C. Kannigadu, D. D. N'Da, *Curr. Pharm. Des.* **2020**, *26*, 4658–4674.
[3] O. Isayev, B. Rasulev, L. Gorb, J. Leszczynski, *Mol. Diversity* **2006**, *10*, 233–245.
[4] H. Stucki, *Chimia* **2004**, *58*, 409–413.
[5] P. Kovacic, R. Somanathan, *J. Appl. Toxicol.* **2014**, *34*, 810–824.
[6] M. Megharaj, B. Ramakrishnan, K. Venkateswarlu, N. Sethunathan, R. Naidu, *Environ. Int.* **2011**, *37*, 1362–1375.
[7] J. C. Spain, *Annu. Rev. Microbiol.* **1995**, *49*, 523–555.
[8] J. S. Strehse, M. Brenner, M. Kisiela, E. Maser, *Arch. Toxicol.* **2020**, *94*, 4043–4054.
[9] M. H. H. Wurzenberger, J. T. Lechner, M. Lommel, T. M. Klapötke, J. Stierstorfer, *Propellants Explos. Pyrotech.* **2020**, *45*, 898–907.
[10] J. W. Fronabarger, M. D. Williams, W. B. Sanborn, D. A. Parrish, M. Bichay, *Propellants Explos. Pyrotech.* **2011**, *36*, 459–470.
[11] T. M. Klapötke, J. T. Lechner, J. Stierstorfer, *Propellants Explos. Pyrotech.* **2022**, *47*, e202100205.
[12] T. M. Klapötke, J. Stierstorfer, M. Weyrauther, T. G. Witkowski, *Chem. Eur. J.* **2016**, *22*, 8619–8626.
[13] J. W. Fronabarger, M. D. Williams, W. B. Sanborn, J. G. Bragg, D. A. Parrish, M. Bichay, *Propellants Explos. Pyrotech.* **2011**, *36*, 541–550.
[14] T. M. Klapötke, P. Mayer, C. Miró Sabaté, J. M. Welch, N. Wiegand, *Inorg. Chem.* **2008**, *47*, 6014–6027.
[15] A. W. Czarnik, *Nature* **1998**, *394*, 417–418.
[16] M. E. Germain, M. J. Knapp, *J. Am. Chem. Soc.* **2008**, *130*, 5422–5423.
[17] T. M. Klapötke, *Chemistry of High-Energy Materials*, 5th ed., De Gruyter, Berlin, Boston, **2019**.
[18] K. D. Oyler, in *Green Energetic Materials*, **2014**, pp. 103–132.
[19] S. J. Toal, W. C. Trogler, *J. Mater. Chem.* **2006**, *16*, 2871–2883.
[20] D. S. Moore, *Rev. Sci. Instrum.* **2004**, *75*, 2499–2512.
[21] V. Merz, G. Zetter, *Ber. Dtsch. Chem. Ges.* **1879**, *12*, 2035–2049.
[22] J. Stenhouse, C. E. Groves, *Ber. Dtsch. Chem. Ges.* **1880**, *13*, 1305–1308.
[23] A. Drechsel, T. M. Klapoetke, T. G. Witkowski, *J. J. Inorg. Chem.* **2016**, *1*, 1–8.
[24] T. G. Witkowski, Dissertation thesis, LMU Munich **2017**.
[25] A. J. Birch, R. A. Massy-Westropp, R. W. Rickards, H. Smith, *J. Chem. Soc.* **1958**, 360–365.
[26] A. P. Marchand, G. M. Reddy, *Synthesis* **1992**, *1992*, 261–262.
[27] M. A. Pierce-Butler, *Acta Crystallogr. Sect. B* **1982**, *38*, 3100–3104.
[28] Y.-G. Bi, Y.-A. Feng, Y. Li, B.-D. Wu, T.-L. Zhang, *J. Coord. Chem.* **2015**, *68*, 181–194.
[29] H. Östmark, S. Wallin, H. G. Ang, *Propellants Explos. Pyrotech.* **2012**, *37*, 12–23.
[30] R. B. Cundall, T. Frank Palmer, C. E. C. Wood, *J. Chem. Soc. Faraday Trans. 1* **1978**, *74*, 1339–1345.
[31] M. Härtel, Dissertation thesis, LMU München **2017**.
[32] W. Acree, J. S. Chickos, *J. Phys. Chem. Ref. Data* **2010**, *39*, 043101.
[33] M. Suceska, *EXPLO5 version V6.05 User's guide*, Zagreb, **2018**.
[34] T. M. Klapötke, *Energetic Materials Encyclopedia, Vol. 1–3*, 2nd ed., DeGruyter, Berlin/Boston, **2021**.
[35] M. H. H. Wurzenberger, B. R. G. Bissinger, M. Lommel, M. S. Gruhne, N. Szimhardt, J. Stierstorfer, *New J. Chem.* **2019**, *43*, 18193–18202.
[36] M. H. H. Wurzenberger, V. Braun, M. Lommel, T. M. Klapötke, J. Stierstorfer, *Inorg. Chem.* **2020**, *59*, 10938–10952.
[37] Impact: insensitive > 40 J, less sensitive ≥ 35 J, sensitive ≥ 4 J, very sensitive ≤ 3 J; Friction: insensitive > 360 N, less sensitive = 360 N, sensitive < 360 N and > 80 N, very sensitive ≤ 80 N, extremely sensitive ≤ 10 N, According to: *Recommendations on the Transport of Dangerous Goods, Manual of Tests and Criteria*, 4th. ed., United Nations, New York-Geneva, **1999**.
[38] M. S. Gruhne, T. Lenz, M. Rösch, M. Lommel, M. H. H. Wurzenberger, T. M. Klapötke, J. Stierstorfer, *Dalton Trans.* **2021**, *50*, 10811–10825.
[39] M. H. H. Wurzenberger, M. S. Gruhne, M. Lommel, N. Szimhardt, T. M. Klapötke, J. Stierstorfer, *Chem. Asian J.* **2019**, *14*, 2018–2028.
[40] N. Szimhardt, M. H. H. Wurzenberger, T. M. Klapötke, J. T. Lechner, H. Reichherzer, C. C. Unger, J. Stierstorfer, *J. Mater. Chem. A* **2018**, *6*, 6565–6577.
[41] N. Szimhardt, M. H. H. Wurzenberger, A. Beringer, L. J. Daumann, J. Stierstorfer, *J. Mater. Chem. A* **2017**, *5*, 23753–23765.
[42] J.-G. Zhang, K. Wang, Z.-M. Li, H. Zheng, T.-L. Zhang, L. Yang, *Main Group Chem.* **2011**, *10*, 205–213.
[43] M. S. Gruhne, M. Lommel, M. H. H. Wurzenberger, N. Szimhardt, T. M. Klapötke, J. Stierstorfer, *Propellants Explos. Pyrotech.* **2020**, *45*, 147–153.
[44] S. M. J. Endraß, T. M. Klapötke, J. Stierstorfer, *New Trends in Research of Energetic Materials* Pardubice, Czech Republic, 06–08 April, **2022**, 311–317.
[45] A. Neuer, G. Bikelyté, S. M. J. Endraß, T. M. Klapötke, J. Stierstorfer, *New Trends in Research of Energetic Materials* Pardubice, Czech Republic, 06–08 April, **2022**, 440–448.

Submitted: August 11, 2022
Accepted: August 15, 2022